Chinese Journal of Electronics
Vol.32, No.5, Sept. 2023

Track-Oriented Marginal Poisson Multi-Bernoulli Mixture Filter for Extended Target Tracking

DU Haocui[1,2], XIE Weixin[1,2], LIU Zongxiang[1,2], and LI Liangqun[1,2]

(1. *ATR Key Laboratory, Shenzhen University, Shenzhen 518060, China*)

(2. *Guangdong Key Laboratory of Intelligent Information Processing, Shenzhen University, Shenzhen 518060, China*)

Abstract — In this paper, we derive and propose a track-oriented marginal Poisson multi-Bernoulli mixture (TO-MPMBM) filter to address the problem that the standard random finite set filters cannot build continuous trajectories for multiple extended targets. First, the Poisson point process model and the multi-Bernoulli mixture (MBM) model are used to establish the set of birth trajectories and the set of existing trajectories, respectively. Second, the proposed filter recursively propagates the marginal association distributions and the Poisson multi-Bernoulli mixture (PMBM) density over the set of alive trajectories. Finally, after pruning and merging process, the trajectories with existence probability greater than the given threshold are extracted as the estimated target trajectories. A comparison of the proposed filter with the existing trajectory filters in two classical scenarios confirms the validity and reliability of the TO-MPMBM filter.

Key words — Extended target tracking, Random finite set, Poisson multi-Bernoulli mixture, Poisson point process, Marginal distribution, Target trajectory.

I. Introduction

Multi-target tracking (MTT) refers to the process of inferring trajectories of an unknown/time-varying number of targets based on the noisy measurement set [1]–[3]. According to the resolution of the sensors and the distances between targets and sensors, the MTT problems can be divided into point MTT and extended target tracking (ETT) [3]. A point target usually assumes that one target generates at most one measurement, while the extended target assumes that a target potentially gives rise to more than one measurement per time step [3]. Compared with the point target which only provides the kinematic state information, the extended target can provide the kinematic state and extent state information, making it more useful in robotics, large ships and car tracking. At present, the widespread applications of modern high-resolution radars make ETT research increasingly become a current research hotspot.

The inhomogeneous Poisson point process (PPP) is a common extended target measurement model. It assumes each extended target generates a Poisson distributed random number of measurements at each time step, and the measurements are spatially distributed around the target [4], [5]. Random finite sets (RFSs) [6] have widely been discussed in the multiple ETT. It provides a theoretical foundation for ETT filters. Based on the PPP model and RFSs theory, the probability hypothesis density (PHD) filter [7], the cardinalised PHD (CPHD) filter [8], the generalized labelled multi-Bernoulli (GLMB) filter [9], the labelled multi-Bernoulli (LMB) filter [10] and the Poisson multi-Bernoulli mixture (PMBM) filter [11] for ETT have been developed.

In RFS-based MTT filters, two conjugate priors [12] are widely used. One is the PMBM conjugate prior, which is based on the unlabelled RFSs; the other is the GLMB conjugate prior, which is based on the labelled RFSs. In accordance with these two conjugate priors, several computationally tractable filters with the closed-form solutions [9]–[15] have been proposed. The available studies have shown that the well-structured PMBM filter with fewer global hypotheses outperforms the GLMB filter in terms of computational time and filtering accuracy [11], [16]. However, the PMBM filter cannot provide target trajectory between time steps [17].

Manuscript Received May 26, 2021; Accepted Oct. 21, 2021. This work was supported by the National Natural Science Foundation of China (61271107, 61703280, 62171287) and the Shenzhen Basic Research Project (JCYJ20170818102503604).

 DOI:10.23919/cje.2021.00.194

To address this problem, two approaches have been developed to build target trajectories. One is to add unique labels to the extended target states and link all the targets with the same label in time series, e.g., the LMB filter, the GLMB filter, and the Delta GLMB (δ-GLMB) filter. The other is to estimate the set of target trajectories instead of the set of target states [17]–[20]. And in this trajectory framework, the filter recursively propagates the posterior trajectory distribution, e.g., the tracker/trajectory PMBM (TPMBM) filter [20].

In this paper, based on the TPMBM filter and the marginal distribution PMBM (MD-PMBM) filter [21], we present the track-oriented marginal PMBM (TO-MPMBM) filter to address the ETT problem. Unlike the TPMBM filter, the proposed filter recursively propagates the the weight, existence probability, and probability density function (pdf) of each track. The experimental results show that the proposed filter outperforms the TPMBM filter and the δ-GLMB filter in terms of the tracking performance and running time.

The rest of the paper is organized as follows: Section II introduces the Bayesian model assumptions, the trajectory RFSs representation, and the trajectory set model; Section III details the recursive process, shape estimation method, complexity analysis and algorithm summary of the TO-MPMBM filter; Section IV tests the proposed tracking algorithm; Section V gives the conclusion.

II. Background

In this section, we introduce several Bayes modeling assumptions, give a brief introduction to the RFSs of the trajectories, and outline the transition and measurement model used in Section III.

1. Bayes modeling assumptions

The target states and sensor measurements are represented as two RFSs in the traditional targets problem formulation [22]. Let X_k denote target state set, and Z_k denote measurement set at time k. Several modeling assumptions are required to establish the multi-extended target transition model and measurement model. They are as follows:

Assumption 1 Given a single target state $x_k \in X_k$, the target either survives with a survival probability $P_s(x_k)$ or disappears with a probability $1 - P_s(x_k)$.

Assumption 2 Each birth target evolves independently of the existing targets, and the birth intensity is given by $D_k^b(x_k)$.

Assumption 3 Each single target state evolves according to the Markov transition function $f(x_k|x_{k-1})$.

Assumption 4 The measurements set Z_k at time k consists of two disjoint sets: the clutter measurement set and the target-generated measurement set, and both sets are independent of each other.

Assumption 5 The clutter can be modeled as a Poisson RFS with Poisson rate λ^{FA} and spatial Poisson distribution $c(z_k)$, and the clutter Poisson intensity is $\kappa(z_k) = \lambda^{\mathrm{FA}} c(z_k)$.

Assumption 6 If the target is detected with probability $P_d(x_k)$, the measurements generated by each target at time step k are a Poisson distribution with Poisson rate γ_k and the spatial distribution $\phi(z_k|x_k)$.

Assumption 7 Given a measurement set w_k, the conditional extended target measurement likelihood when w_k is a nonempty set (detected) and an empty set [11] can be expressed as follows:

$$l_{\mathrm{w}_k}(x_k) = P_d(x_k)\mathrm{e}^{-\gamma(x_k)} \prod_{z_k \in \mathrm{w}_k} \gamma(x_k)\phi(z_k|x_k) \tag{1}$$

$$\begin{aligned} l_{\emptyset}(x_k) &= 1 - P_d(x_k)(1 - \mathrm{e}^{-\gamma(x_k)}) \\ &= 1 - P_d(x_k) + P_d(x_k)\mathrm{e}^{-\gamma(x_k)} \end{aligned} \tag{2}$$

where $1 - \mathrm{e}^{-\gamma(x_k)}$ denotes the extended target generating at least one measurement and $P_d(x_k)(1 - \mathrm{e}^{-\gamma(x_k)})$ is the effective detection probability of an extended target.

2. RFSs of trajectory

Let $\mathcal{X}$ denote the single-target state space. Similar to the trajectory state model [18], the trajectory state model used in this paper is a tuple $X = (\beta, \varepsilon, x_{\beta:\varepsilon})$, in which β is the time step at which a trajectory starts, ε is the time step at which the trajectory ends. If the current time is k, $\varepsilon = k$ means the trajectory is still alive. For each specific trajectory, its sequence of states is $x_\beta, x_{\beta+1}, \ldots, x_{\varepsilon-1}, x_\varepsilon$, its length is $l = \varepsilon - \beta + 1$. The trajectory state space [19] $\mathcal{T}_k$ at time k is given by

$$\mathcal{T}_k = \biguplus_{(\beta,\varepsilon)\in I_k} \{\beta\} \times \{\varepsilon\} \times \mathcal{X}^{\varepsilon-\beta+1} \tag{3}$$

where $\uplus$ denotes the union of disjoint sets $I_k = \{(\beta, \varepsilon) : 0 \le \beta \le \varepsilon \le k\}$ and $\mathcal{X}^{\varepsilon-\beta+1}$ denotes the Cartesian products. If $\varepsilon \ge \beta$, the trajectory state density of X_k at time step k can be written as

$$\pi_{k|k'}(X_k) = \pi_{k|k'}(x_{\beta:\varepsilon}|\beta, \varepsilon) P_{k|k'}(\beta, \varepsilon), \quad k' \le k \tag{4}$$

Otherwise, $\pi_{k|k'}(X_k) = 0$. The integration of a single trajectory density can be written as

$$\begin{aligned} &\int \pi(X)\mathrm{d}X \\ &= \sum_{\beta,\varepsilon} \left[\int \cdots \int \pi(x_\beta, \ldots, x_\varepsilon|\beta, \varepsilon)\mathrm{d}x_\beta \cdots \mathrm{d}x_\varepsilon \right] P(\beta, \varepsilon) \end{aligned} \tag{5}$$

Let $\mathrm{X}_k \in \mathcal{F}(\mathcal{T}_k)$ denote the set of trajectories up to

time k where $\mathcal{F}(\mathcal{T}_k)$ is the set of all subsets of $\mathcal{T}_k$, and $g(\mathrm{X}_k)$ denotes a real-valued function on a set of trajectories. The set integral is given by

$$\begin{aligned}&\int g(\mathrm{X}_k)\mathrm{d}\mathrm{X}_k\\&=g(\emptyset)\\&\quad+\sum_{n=1}^{\infty}\frac{1}{n!}\int\cdots\int g(\{X_k^1,\ldots,X_k^n\})\mathrm{d}X_k^1\ldots\mathrm{d}X_k^n\end{aligned}\tag{6}$$

where $\mathrm{X}_k=\{X_k^1,\ldots,X_k^n\}$, $g(\mathrm{X}_k)$ denotes the multi-trajectory density of an RFS of trajectories, and $\int g(\mathrm{X}_k)\mathrm{d}\mathrm{X}_k=1$ for $g(\mathrm{X}_k)\geq 0$.

In analogy to the definition for the set of targets density function, $f(\mathrm{X})$ denotes the set of the trajectory density function. The probability generating functional (p.g.fl.) [6] can simplify the analysis of RFSs that possess independence relationships and is a useful tool for understanding RFS densities. The p.g.fl. for a trajectory RFS density can be defined as

$$G[h]=\int h^{\mathrm{X}}f(\mathrm{X})\mathrm{d}\mathrm{X}\tag{7}$$

where $h^{\mathrm{X}}=\prod_{X\in\mathrm{X}}h(X)$ is set power.

The RFS-based MTT approach consists of two major parts: the Poisson RFS and the Bernoulli RFS. We use the Bernoulli RFS to model the existing alive trajectory density, and the Poisson RFS to model the birth and missed detection trajectory density. The density and the corresponding p.g.fl. of a trajectory Bernoulli are given by

$$f^{\mathrm{ber}}(\mathrm{X})=\begin{cases}1-r, & \mathrm{X}=\emptyset\\ rf(X), & \mathrm{X}=\{X\}\\ 0, & \text{otherwise}\end{cases}\tag{8}$$

$$G^{\mathrm{ber}}[h]=1-r+r\langle f;h\rangle\tag{9}$$

where $f(X)$ is the probability density function of a single existence-conditional trajectory, r is the Bernoulli existence probability, $\langle f;h\rangle$ is the inner product of $f(\cdot)$ and $h(\cdot)$, i.e., $\langle f;h\rangle=\int f(X)h(X)\mathrm{d}X$ and $\langle f;h-1\rangle=\int f(X)h(X)\mathrm{d}X-\int f(X)\mathrm{d}X$. The appearance and disappearance of a target trajectory can be measured by $f(X)$ and r. Similar to definitions of the target multi-Bernoulli RFS and the target multi-Bernoulli mixture (MBM) RFS, the trajectory multi-Bernoulli RFS and the trajectory MBM RFS can be described as: A trajectory multi-Bernoulli denotes the disjoint union of a multiple trajectory Bernoulli RFS; the trajectory MBM RFS means an RFS whose density is a mixture of the trajectory multi-Bernoulli densities.

When X_i is an independent trajectory Bernoulli process, the RFS density and p.g.fl. of a trajectory multi-Bernoulli process resulting from the union $\mathrm{X}=\bigcup_{i=1}^{N}\mathrm{X}_i$ can be written as

$$G_{\mathrm{X}}[h]=\prod_{i=1}^{N}(1-r_i+r_i\langle f_i;h\rangle)\tag{10}$$

$$\begin{aligned}&f^{\mathrm{ber}}(\mathrm{X})\\&=\left[\prod_{i=1}^{N}(1-r_i)\right]\cdot\sum_{1\leq i_1\leq i_2\leq\cdots\leq i_n\leq N}\prod_{j=1}^{n}\left[\frac{r_{i_j}}{1-r_{i_j}}f_{i_j}(X_i)\right]\\&=\sum_{\alpha\in P_N^n}\prod_{i=1}^{N}f_i(\mathrm{X}_{\alpha(i)})\end{aligned}\tag{11}$$

$$\begin{aligned}P_N^n=&\big\{\alpha:\{1,2,\ldots,N\}\to\{0,1,\ldots,n\}|\\&\{1,\ldots,n\}\subset\alpha(\{1,2,\ldots,N\}),\\&\text{and if }\alpha(i)>0,i\neq j,\text{ then }\alpha(i)\neq\alpha(j)\big\}\end{aligned}\tag{12}$$

$$\mathrm{X}_{\alpha(i)}=\begin{cases}\emptyset, & \alpha(i)=0\\ \{X_{\alpha(i)}\}, & \alpha(i)>0\end{cases}\tag{13}$$

where $f_i(\mathrm{X}_{\alpha(i)})$ is the density of a trajectory Bernoulli of the form (8) with parameters r_i and $f_i(X)$, P_N^n is the set of all functions.

The density and the corresponding p.g.fl. of a trajectory Poisson RFS are given by

$$f^p(\mathrm{X})=\mathrm{e}^{-\int D(X')dX'}\prod_{X\in X}D(X)\tag{14}$$

$$G^p[h]=\exp\{\langle D;h-1\rangle\}\propto\exp\{\langle D;h\rangle\}\tag{15}$$

where $D(X)$ is the trajectory Poisson RFS intensity that is defined on the the trajectory state space $\mathcal{T}_k$.

3. Models for sets of trajectories

1) Transition models for the set of trajectories

In the multi-target transition model, the birth target can be modeled as a Poisson RFS with birth intensity

$$D_k^B(X)=D_{k,x}^B(x_{\beta:\varepsilon}|\beta,\varepsilon)\delta_{k,\varepsilon}\delta_{k,\beta}\tag{16a}$$

$$D_{k,x}^B(x_{k:k}|k,k)=D_k^b(x_k)\tag{16b}$$

where $\delta_{i,j}$ denotes Kronecker delta function.

In this paper, we focus our attention on the set of alive trajectories [17] that are still alive in the surveillance area at the current time step, i.e., $0\leq\beta\leq\varepsilon=k$.

The survival probability of each track is defined as

$$P_{s,k}(X)=P_s(x_\varepsilon)\delta_{k,\varepsilon}\tag{17}$$

The Bernoulli RFS transition density [20] without birth is given by

$$f^{\text{ali}}_{k|k-1}(\mathrm{X}|\mathrm{X}')=\begin{cases}1, & \mathrm{X}'=\emptyset,\mathrm{X}=\emptyset\\ 1-P_{s,k-1}(X'), & \mathrm{X}'=\{X'\},\mathrm{X}=\emptyset\\ P_{s,k-1}(X')f^{\text{ali}}(X|X'), & \mathrm{X}'=\{X'\},\mathrm{X}=\{X\}\\ 0, & \text{otherwise}\end{cases} \tag{18a}$$

$$f^{\text{ali}}(X|X')=f^{\text{ali}}_{x}(x_{\beta:\varepsilon}|\beta,\varepsilon,X')\delta_{\varepsilon'+1,\varepsilon}\delta_{\beta',\beta} \tag{18b}$$

$$f^{\text{ali}}_{x}(x_{\beta:\varepsilon}|\beta,\varepsilon,X')=f_x(x_\varepsilon|x'_{\varepsilon'})\delta_{x'_{\beta':\varepsilon'}}(x_{\beta:\varepsilon-1}) \tag{18c}$$

where $\delta(\cdot)$ denotes the Dirac delta function. In this model, a target may die or be alive. If a target dies, its trajectory will be removed; otherwise, its trajectory will be extended to the next time step. The p.g.fl. of the multiple extended targets transition density can be written as

$$\begin{aligned}&G^{\text{ali}}_{k|k-1}[h|\mathrm{X}']\\&=\int h^X f^{\text{ali}}_{k|k-1}(\mathrm{X}|\mathrm{X}')\mathrm{d}\mathrm{X}\\&=\exp\{\langle D^B_k;h-1\rangle\}(1-P_{s,k-1}+P_{s,k-1}\langle f^{\text{ali}};h\rangle)^{\mathrm{X}'}\end{aligned} \tag{19}$$

For the above transition model, the union of the birth process (PPP RFS) and the set of trajectories (Bernoulli RFS) generated from the previous set of trajectories constitutes the predicted set of trajectories.

2) Single trajectory measurement model

The extended target measurement model can be defined as a Bernoulli measurement density with

$$l_{\mathrm{w}_k}(X)=l_{\mathrm{w}_k}(x_\varepsilon)\delta_{k,\varepsilon} \tag{20a}$$

$$\varphi_k(\mathrm{w}_k|\mathrm{X})=\begin{cases}1, & \mathrm{X}=\emptyset,\quad \mathrm{w}_k=\emptyset\\ l_\emptyset(X), & \mathrm{X}=\{X\},\mathrm{w}_k=\emptyset\\ l_{\mathrm{w}_k}(X), & \mathrm{X}=\{X\},\mathrm{w}_k\neq\emptyset\\ 0, & \text{otherwise}\end{cases} \tag{20b}$$

Equation (20b) implies that an extended target can be detected iff $\varepsilon=k$. The measurement p.g.fl. is

$$G_k[g|\mathrm{X}_k]=\exp\{\langle\lambda^{\text{FA}}_k;g-1\rangle\}(1-P_d+P_d\langle\phi;g\rangle)^{\mathrm{X}_k} \tag{21}$$

III. TO-MPMBM Filter

Based on the TPMBM filter [20] and the MD-PMBM filter [21], the multiple trajectories (MBM component) can be decomposed into the distributions of multiple single trajectories, and the distribution of each single trajectory can be calculated from the marginal distribution by equation (22f), hence the proposed filter can be referred to as the TO-MPMBM filter. The trajectory marginal PMBM density and its corresponding p.g.fl. can be defined as

$$f_{k|k'}(\mathrm{X}_k)=\sum_{\mathrm{X}^u_k\uplus\mathrm{X}^d_k=\mathrm{X}_k}f^{\text{ppp}}_{k|k'}(\mathrm{X}^u_k)f^{\text{mbm}}_{k|k'}(X^d_k) \tag{22a}$$

$$G_{k|k'}[h]=G^{\text{ppp}}_{k|k'}[h]G^{\text{mbm}}_{k|k'}[h] \tag{22b}$$

$$f^{\text{ppp}}_{k|k'}(\mathrm{X}^u_k)=\exp\left\{-\int D^u_{k|k'}(X')\mathrm{d}X'\right\}\prod_{X\in\mathrm{X}^u_k}D^u_{k|k'}(X) \tag{22c}$$

$$G^{\text{ppp}}_{k|k'}[h]=\exp\left\{\langle D^u_{k|k'};h-1\rangle\right\} \tag{22d}$$

$$f^{\text{mbm}}_{k|k'}(\mathrm{X}^d_k)=\sum_{\alpha\in P_N^{|\mathrm{X}^d_k|}}\prod_{i\in\mathbb{T}_{k|k'}}f^{d,i}_{k|k'}(\mathrm{X}_{\alpha(i)}) \tag{22e}$$

$$f^{d,i}_{k|k'}(\mathrm{X}_{\alpha(i)})=\sum_{a^i\in\mathcal{H}^i_{k|k'}}\omega^{d,i,a^i}_{k|k'}f^{d,i,a^i}_{k|k'}(\mathrm{X}_{\alpha(i)}) \tag{22f}$$

$$G^{\text{mbm}}_{k|k'}[h]=\sum_{a\in\mathcal{A}_{k|k'}}\prod_{i\in\mathbb{T}_{k|k'}}\omega^{d,a}G^{d,i,a^i}_{k|k'}[h] \tag{22g}$$

where the set of trajectories X_k is the disjoint union of a Poisson RFS X^u_k (which represents the unknown target trajectories that are hypothesized to exist but have not detected yet, e.g., the new birth target trajectories and the undetected target trajectories at the current time) with intensity $D^u_{k|k'}(\cdot)$ and an MBM RFS X^d_k with Bernoulli parameters $r^{d,i,a^i}_{k|k'}$ and $f^{d,i,a^i}_{k|k'}(\cdot)$, cf. equation (8); $P_N^{|\mathrm{X}^d_k|}$ and $X_{\alpha(i)}$ are defined in (12) and (13); $\mathcal{A}_{k|k'}$ is the set of global data association history hypotheses, each global hypothesis contains a single trajectory hypothesis from each track. For each track, there are $h^i_{k|k'}$ single trajectory hypotheses. In equation (22a), if $k'=k-1$, then $f_{k|k'}(\mathrm{X}_k)=f_{k|k-1}(\mathrm{X}_k)=f_{k|k-1}(\mathrm{X}_k|\mathrm{Z}^{k-1})$ (Z^{k-1} is the set of measurements up to and including time $k-1$) denotes the predicted distribution; else if $k'=k$, then $f_{k|k'}(\mathrm{X}_k)=f_{k|k}(\mathrm{X}_k)=f_{k|k}(\mathrm{X}_k|\mathrm{Z}^k)$ denotes the updated distribution. In the MBM RFS of (22g), $\mathbb{T}_{k|k'}$ is a track table with $n_{k|k'}$ tracks; $a\in\mathcal{A}_{k|k'}$ is a global data association hypothesis for each global hypothesis a and each track $i\in\mathbb{T}_{k|k'}$, a^i indicates which local track hypothesis is used in the global hypothesis.

The global data association hypothesis weights are correlated with single trajectory hypothesis weights

$$\omega^{d,a}\propto\prod\nolimits_{i\in\mathbb{T}_{k|k'}}\omega^{d,i,a^i}_{k|k'} \tag{23}$$

where $\omega^{d,i,a^i}_{k|k'}$ denotes the trajectory marginal association distribution for track i. The normalized $\omega^{d,a}$ satisfies $\sum_{a\in\mathcal{A}_{k|k'}}\omega^{d,a}=1$.

Let m_k be the number of measurements Z_k at time k and $j\in\mathbb{M}_k=\{1,2,\ldots,m_k\}$ be the index of each corresponding measurement. $\mathcal{M}_k$ represents the tuples set (t,j) that satisfies $t\leq k$ and $j\in\mathbb{M}_t$; and $\mathcal{M}_k(i,a^i)\subseteq$

$\mathcal{M}_k$ denotes the history of measurements that are related to track i in hypothesis a^i. Since each extended target generates at least one measurement at each time step, $\mathcal{M}_k(i,a^i)$ contains more than one element at time step k, as shown in Example 1. Each global hypothesis needs to explain the origin of each measurement, so $\mathcal{A}_{k|k'}$ can be defined as

$$\begin{aligned}\mathcal{A}_{k|k'} = \big\{&(a^1,a^2,\ldots,a^{n_{t|t'}})|a^i\in\mathcal{H}^i_{k|k'},\\ &\bigcup\nolimits_{i\in\mathbb{T}_{k|k'}}\mathcal{M}_{k'}(i,a^i)=\mathcal{M}_{k'},\\ &\mathcal{M}_{k'}(i,a^i)\cap\mathcal{M}_{k'}(j,a^j)=\emptyset,\ \ \forall i\neq j\big\}\end{aligned}\tag{24}$$

Example 1 If $\mathcal{M}_5(i,a^i)=\{(2,1),(2,2),(2,3),(4,5),(5,9)\}$, then a^i hypothesis indicates that the i-th hypothesized target is first detected at time 2 by measurement 1, 2, and 3, missed detection occurs at time 3, it is detected at time 4 by measurement 5, and it is detected at time 5 by measurement 9.

In the TO-MPMBM filter, the Bernoulli existence probability r denotes the probability of a trajectory that is still alive. The prediction and update for the set of alive trajectories are as follows:

1. Prediction

Theorem 1 Given the set of alive trajectories distribution at time step $k-1$ (see (22)), the transition model (18) and the birth model (16), the predicted distribution is a trajectory marginal PMBM with

$$\begin{aligned}&D^u_{k|k-1}(X_k|X_{k-1})\\&=D^B_k(X_k)\\&\quad+\int D^u_{k-1|k-1}(X_{k-1})P_{s,k-1}(X_{k-1})f^{\text{ali}}(X_k|X_{k-1})\mathrm{d}X_{k-1}\end{aligned}\tag{25a}$$

$$n_{k|k-1}=n_{k-1|k-1}\tag{25b}$$

$$h^i_{k|k-1}=h^i_{k-1|k-1}\tag{25c}$$

$$\omega^{d,i,a^i}_{k|k-1}=\omega^{d,i,a^i}_{k-1|k-1},\forall a^i\tag{25d}$$

$$\begin{aligned}&r^{d,i,a^i}_{k|k-1}\\&=r^{d,i,a^i}_{k-1|k-1}\int f^{d,i,a^i}_{k-1|k-1}(X_{k-1})P_{s,k-1}(X_{k-1})\mathrm{d}X_{k-1},\ \forall a^i\end{aligned}\tag{25e}$$

$$\begin{aligned}&f^{d,i,a^i}_{k|k-1}(X_k)\\&=\frac{\int f^{d,i,a^i}_{k-1|k-1}(X_{k-1})P_{s,k-1}(X_{k-1})f^{ali}(X_k|X_{k-1})\mathrm{d}X_{k-1}}{\int f^{d,i,a^i}_{k-1|k-1}(X_{k-1})P_{s,k-1}(X_{k-1})\mathrm{d}X_{k-1}},\ \forall a^i\end{aligned}\tag{25f}$$

The proof is given in Appendix A.

2. Update

To find the measurements generated by each extended target, the measurement set needs to be partitioned. In this paper, the power set $\mathcal{P}(\mathrm{Z}_k)$ of Z_k denotes all partitions of the measurement set Z_k, w^p_k denotes the p-th ($p\in\{1,\ldots,|\mathcal{P}(\mathrm{Z}_k)|-1\}$) nonempty partition in $\mathcal{P}(\mathrm{Z}_k)$ and $|\mathrm{w}^p_k|$ is the number of measurement set cells in this partition, i.e., $\{j_1,j_2,\ldots,j_{|\mathrm{w}^p_k|}\}$ denotes the set of measurement indices of w^p_k.

Theorem 2 Given the predicted trajectory distribution (18), the single trajectory measurement model (20) and (21), and the clutter with the Poisson intensity $\kappa(z_k)$ (Assumption 5), the updated distribution is a trajectory marginal PMBM with

$$D^u_{k|k}(X_k)=l_\emptyset(X_k)D^u_{k|k-1}(X_k|X_{k-1})\tag{26}$$

$$n_{k|k-1}=n_{k-1|k-1}+|\mathcal{P}(\mathrm{Z}_k)|-1\tag{27}$$

$$\mathcal{M}_k=\mathcal{M}_{k-1}\cup\{(k,j_1),(k,j_2),\ldots,(k,j_{|\mathrm{w}^p_k|})\}\tag{28}$$

For the tracks ($i\in\{1,\ldots,n_{k|k-1}\}$) continuing from the previous time step, the hypotheses at time step k originate from three cases: from time step $k-1$, from the missed detection, or from an update with a nonempty measurement set w^p_k. At time step k, there are $h^i_{k|k}=|\mathcal{P}(\mathrm{Z}_k)|h^i_{k|k-1}$ hypotheses.

Case 1 Update existing tracks ($i\in\{1,\ldots,n_{k|k-1}\}$, $\tilde{a}^i\in\{1,\ldots,h^i_{k|k-1}\}$, $\tilde{a}^i$ is the previous hypothesis) with the nonempty measurement set w^p_k:

$$a^i=\tilde{a}^i+h^i_{k|k-1}p\tag{29a}$$

$$\begin{aligned}\mathcal{M}_k(i,a^i)=&\mathcal{M}_{k-1}(i,\tilde{a}^i)\\&+\{(k,j_1),(k,j_2),\ldots,(k,j_{|\mathrm{w}^p_k|})\}\end{aligned}\tag{29b}$$

$$\omega^{d,i,a^i}_{k|k}=\omega^{d,i,a^i}_{k|k-1}r^{d,i,\tilde{a}^i}_{k|k-1}\int f^{d,i,\tilde{a}^i}_{k|k-1}(X_k)l_{\mathrm{w}^p_k}(X_k)\mathrm{d}X_k\tag{29c}$$

$$r^{d,i,a^i}_{k|k}=1\tag{29d}$$

$$f^{d,i,a^i}_{k|k}(X_k)=\frac{l_{\mathrm{w}^p_k}(X_k)f^{d,i,\tilde{a}^i}_{k|k-1}(X_k)}{\int f^{d,i,\tilde{a}^i}_{k|k-1}(X_k)l_{\mathrm{w}^p_k}(X_k)\mathrm{d}X_k}\tag{29e}$$

Case 2 Update tracks ($i\in\{1,\ldots,n_{k|k-1}\}$, $a^i\in\{1,\ldots,h^i_{k|k-1}\}$) using the missed detection hypotheses:

$$\mathcal{M}_k(i,a^i)=\mathcal{M}_{k-1}(i,a^i)\tag{30a}$$

$$\begin{aligned}\omega^{d,i,a^i}_{k|k}=&\omega^{d,i,a^i}_{k|k-1}(1-r^{d,i,a^i}_{k|k-1}\\&+r^{d,i,a^i}_{k|k-1}\int l_\emptyset(X_k)f^{d,i,a^i}_{k|k-1}(X_k)\mathrm{d}X_k)\end{aligned}\tag{30b}$$

$$r^{d,i,a^i}_{k|k}=\frac{r^{d,i,a^i}_{k|k-1}\int l_\emptyset(X_k)f^{d,i,a^i}_{k|k-1}(X_k)\mathrm{d}X_k}{1-r^{d,i,a^i}_{k|k-1}+r^{d,i,a^i}_{k|k-1}\int l_\emptyset(X_k)f^{d,i,a^i}_{k|k-1}(X_k)\mathrm{d}X_k}\tag{30c}$$

$$f_{k|k}^{d,i,a^i}(X_k)=\frac{l_{\emptyset}(X_k)f_{k|k-1}^{d,i,a^i}(X_k)}{\int l_{\emptyset}(X_k)f_{k|k-1}^{d,i,a^i}(X_k)\mathrm{d}X_k} \tag{30d}$$

Case 3 Update new tracks($i\in\{n_{k|k-1}+p\}$) with the nonempty measurement set w_k^p:

$$h_{k|k}^{i}=2 \tag{31a}$$

$$\mathcal{M}_k(i,1)=\emptyset,\omega_{k|k}^{d,i,1}=1,r_{k|k}^{d,i,1}=0 \tag{31b}$$

$$\mathcal{M}_k(i,2)=\{(k,j_1),(k,j_2),\ldots,(k,j_{|\mathrm{w}_k^p|})\} \tag{31c}$$

$$\omega_{k|k}^{d,i,2}=\begin{cases}\kappa(\mathrm{w}_k^p)+\int D_{k|k-1}^{u}(X_k)l_{\mathrm{w}_k^p}(X_k)\mathrm{d}X_k, & |\mathrm{w}_k^p|=1\\ \int D_{k|k-1}^{u}(X_k)l_{\mathrm{w}_k^p}(X_k)\mathrm{d}X_k, & |\mathrm{w}_k^p|>1\end{cases} \tag{31d}$$

$$r_{k|k}^{d,i,2}=\begin{cases}\dfrac{\int D_{k|k-1}^{u}(X_k)\,l_{\mathrm{w}_k^p}(X_k)\mathrm{d}X_k}{\kappa(\mathrm{w}_k^p)+\int D_{k|k-1}^{u}(X_k)l_{\mathrm{w}_k^p}(X_k)\mathrm{d}X_k}, & |\mathrm{w}_k^p|=1\\ 1, & |\mathrm{w}_k^p|>1\end{cases} \tag{31e}$$

$$f_{k|k}^{d,i,2}(X_k)=\frac{D_{k|k-1}^{u}(X_k)l_{\mathrm{w}_k^p}(X_k)}{\int D_{k|k-1}^{u}(X_k)l_{\mathrm{w}_k^p}(X_k)dX_k} \tag{31f}$$

With the help of Appendixes B and C, the proof of Theorem 2 is given in Appendix D.

The above single trajectory and the intensity of the Poisson RFS can be given as a mixture density of the form

$$\pi(X)=\sum\nolimits_j \omega^j\pi^i(x_{\beta:\varepsilon}|\beta,\varepsilon)\delta_{e^j,\varepsilon}\delta_{b^j,\beta} \tag{32}$$

where each mixture density consists of a weight ω^j, a birth time b^j, a recent time e^j, $b^j\le e^j$, and a state sequence density $\pi^i(\cdot)$ for $\forall j$.

3. Shape estimation method

For the general ETT algorithms, in addition to the above prediction and update steps, the shape of each extended target needs to be estimated. Scholars have proposed many shape estimation methods. The representative methods include the random matrix (RM) [7], [23]–[25] (or Gamma Gaussian inverse Wishart (GGIW) [8]–[11], [20]), random hypersurface (RH) [26], [27], and Gaussian process (GP) [28], etc. Since the GGIW method is particularly easy to integrate into common ETT algorithms, such as the CPHD filter [8] and the PMBM filter [11], we employ the GGIW method to estimate the shape of extended targets. In this paper, we focus on deriving the prediction and update of the TO-MPMBM filter, hence the shape estimation is only briefly discussed (detailed in [11]).

4. Discussion

The above analysis shows that the TO-MPMBM filter recursively propagates the prediction and the update of the set of alive trajectories. Each track corresponds to a hypothesis tree, and each hypothesis is a sequence of different data associations for the track, as shown in Fig.1 where the numbers of measurements at time steps 1 and 2 are 1 and 2, respectively, and the line with arrow constitutes a valid global hypothesis. As time goes on, the number of data associations [29], global hypotheses, and MBM components are exponential increasing, which leads to a huge computational burden.

To reduce the complexity of data associations, reduction methods, such as gating, clustering [10], [11], [30], random sampling [29], [31], [32], pruning, merging, and recycling, are widely used in the point MTT algorithms and the ETT algorithms. In the proposed TO-MPMBM filter, we use the random sampling method to maximize the data association likelihood. Besides, for the up-

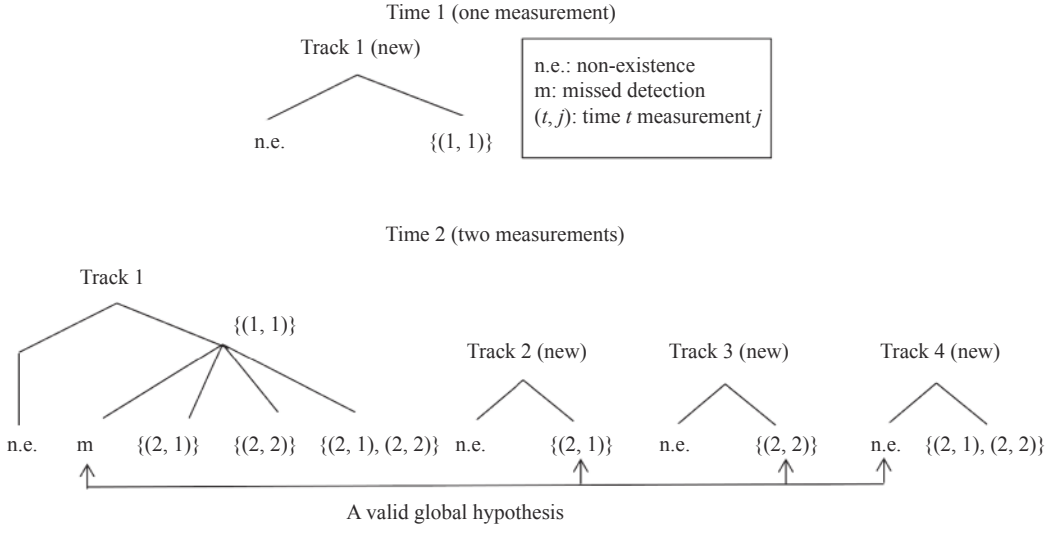

Fig. 1. Tracks and hypotheses of the TO-MPMBM filter.

dated marginal PMBM density of each track, global hypotheses with weight lower than the given threshold are pruned, and Bernoulli components with existence probability lower than the given threshold are removed.

In the implementation of the TO-MPMBM filter, global hypotheses are represented by a look-up table, in which, the (j, i)-th element corresponds to the index of the j-th global hypothesis including the single trajectory hypothesis in the i-th track. If the i-th single trajectory hypothesis does not include in the j-th global hypothesis, the (j, i)-th element equals zero.

Example 2 As shown in Fig.1, there are four valid global hypotheses at time step 2. Assuming the single trajectory hypotheses in each track are indexed from left to right, the corresponding global look-up table is

$$\begin{bmatrix} 1 & 1 & 1 & 0 \\ 2 & 1 & 0 & 0 \\ 3 & 0 & 0 & 0 \\ 4 & 0 & 0 & 0 \end{bmatrix} \tag{33}$$

5. Pseudo code of the TO-MPMBM filter

Based on the GGIW method [11], the pseudo code for one step prediction and update of the extended target TO-MPMBM filter is given in Algorithm 1.

Algorithm 1 Pseudo code of one prediction and update for extended target TO-MPMBM filter

Input: Parameters of the trajectory marginal PMBM posterior, the global hypotheses look-up table at time k-1 and the measurement set Z_k.

Output: Parameters of the trajectory marginal PMBM posterior and the global hypotheses look-up table at time k.

1: Calculate the predicted PPP intensity $D^u_{k|k-1}(\cdot)$ via equation (25a) to predict the existing PPP (missed or pruned GGIW components) and the birth PPP;

2: **for** $i = 1, \ldots, n_{k-1|k-1}$ **do**
  for $a^i = 1, \ldots, h^i_{k-1|k-1}$ **do**
    Predict $\omega^{d,i,a^i}_{k|k-1}$, $r^{d,i,a^i}_{k|k-1}$ and $f^{d,i,a^i}_{k|k-1}(\cdot)$ via (25d)–(25f);
  end for
end for

3: **for** $z \in \mathrm{Z}_k$ **do**
  Calculate the gated measurements of undetected targets and detected targets by gating each mixture component of Poisson intensity and each single trajectory density contained in Bernoulli RFS;
end for

4: **for** $a \in \mathcal{A}_{k|k-1}$ **do**

4.1: Calculate the subset $\mathcal{P}(\mathrm{Z}_k)$ of the data association by partitioning the set of measurements within the gate of existing targets;

4.2: Reduce the number of data association subsets by normalizing and pruning multi-Bernoulli with low weights, and prune measurement partitions that correspond to low weight global hypotheses indices of measurements that have been associated to pre-existing targets;

  for $i = 1, \ldots, n_{k|k-1}$ **do**
    for $a^i = 1, \ldots, h^i_{k|k-1}$ **do**
      if $w^p_k \neq \emptyset$ **then**

4.3: Update $\omega^{d,i,a^i}_{k|k}$, $r^{d,i,a^i}_{k|k}$ and $f^{d,i,a^i}_{k|k}(\cdot)$ via (29c)–(29e), i.e., create new Bernoulli components by updating the hypotheses of the existing trajectories;

      else

4.4: Update $\omega^{d,i,a^i}_{k|k}$, $r^{d,i,a^i}_{k|k}$ and $f^{d,i,a^i}_{k|k}(\cdot)$ via (30b)–(30d), i.e., create new Bernoulli components by updating the missed detection hypotheses;

      end if
    end for
  end for
  for $i \in \{n_{k|k-1} + p\}$ **do**

4.5: Update $\omega^{d,i,a^i}_{k|k}$, $r^{d,i,a^i}_{k|k}$ and $f^{d,i,a^i}_{k|k}(\cdot)$ via (31), i.e., create new Bernoulli components by updating new tracks;

  end for

4.6: Prune global hypotheses with weight lower than a threshold and update hypotheses look-up table;

4.7: Prune Bernoulli components whose existence probability is below a threshold or do not appear in the truncated global hypotheses and update hypotheses look-up table;

end for

5: Merge duplicate global hypotheses and update hypotheses look-up table;

6: Update the Poisson intensity for measurements that only fall inside the gate of undetected targets via (26) and the clustering method;

7: Prune PPP components with weights smaller than a given threshold;

8: Estimate the set of alive trajectories;

9: Recycle Bernoulli components pruned in step 4 and add them to PPP components.

IV. Simulation

In this section, the proposed TO-MPMBM filter is compared with two typical extended target trajectory filters [9], [20] in two scenarios [9]–[11], [33] in terms of the tracking performance and running time.

Each extended target state consists of three variables, the measurement rate γ_k, the kinematic state x_k, and the extent state E_k, that is $\xi^{(i)}_k = \{\gamma^{(i)}_k, x^{(i)}_k, E^{(i)}_k\}$, where $x_k = [p_k, v_k]^{\mathrm{T}} \in \mathbb{R}^4$, $p_k \in \mathbb{R}^2$ is the position, $v_k \in \mathbb{R}^2$ is the velocity and $E_k \in \mathbb{S}^2_{++}$. The motion model, the measurement model, and their corresponding parameters can be defined as

$$\gamma_{k+1} = \gamma_k \tag{34}$$

$$x_{k+1} = f(x_k) + w_k \tag{35}$$

$$E_{k+1} = M(x_k) E_k M(x_k)^{\mathrm{T}} \tag{36}$$

$$z_k = H_k x_k + \upsilon_k \tag{37}$$

$$f(x_k) = \begin{bmatrix} I_2 & T_s I_2 \\ 0 & I_2 \end{bmatrix} x_k, \quad Q = G\sigma_a^2 I_2 G^{\mathrm{T}} \tag{38}$$

$$G = \begin{bmatrix} \frac{T_s^2}{2} I_2 \\ T_s I_2 \end{bmatrix}, \quad H_k = [I_2 \ \ 0_2] \tag{39}$$

where w_k is the Gaussian process noise with zero mean and covariance Q; $f(\cdot)$ and $M(\cdot)$ are the transition matrix of kinematic state and extent state, respectively; H_k is the measurement matrix, and υ_k is the Gaussian observation noise with zero mean and covariance E_k; σ_a is the acceleration standard deviation and $T_s = 1$ s. Given that the kinematic state motion model is a model with constant velocity, the extent transition function $M(\cdot)$ is an identity matrix. The measurement model is also linear Gaussian in a two-dimensional Cartesian coordinate system.

The process of obtaining estimates of the set of trajectories (or set of states) from the multi-target density is called trajectory (or state) extraction. The δ-GLMB filter needs performing state extraction at each time step and then connects target states with the same label to form target state trajectories, see [9]. For the TO-MPMBM filter and the TPMBM filter, an estimate of the set of trajectories is extracted from MBM components with the highest weight and existence probability larger than 0.5.

To evaluate the tracking performance of the three algorithms, we use the generalized optimal sub-pattern assignment (GOSPA) metric [34], and the distance measurement used in the GOSPA metric is the Gaussian Wasserstein Distance metric [35]. The parameters used in GOSPA metric are: the location error cutoff $c = 10$, the ordered $p = 1$, and the track switch cost $s = 4$. Besides, we divide the GOSPA metric into four categories: localization/ extended error (LEE), false detection error (FDE), miss detection error (MDE), and track switch error (SE). The trajectory extraction method of the three algorithms used in this paper is given in [20].

1. The high clutter scenario

In this scenario, there are 100 time steps, 27 highly time-varying numbers of extended targets are randomly generated in four fixed positions ($[\pm 75, \pm 75]^{\mathrm{T}}$), as shown in Fig.2. Table 1 shows the target detection probability P_d, the target survival probability P_s, the clutter Poisson rate λ, and the measurement Poisson rate γ for the three filters. This scenario aims to test the three algorithms' tracking performance in case of a high clutter density and high target numbers.

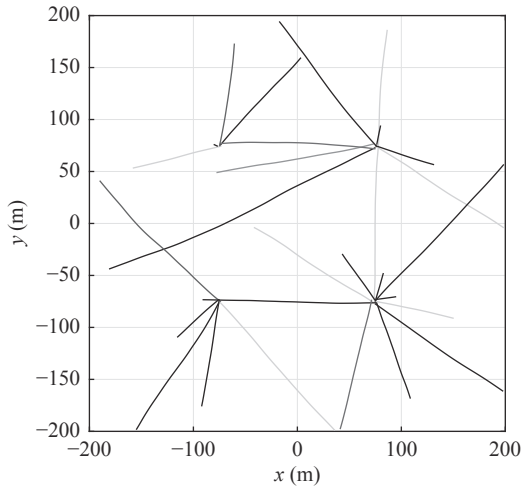

Fig. 2. Target trajectories.

Table 1. The parameters

P_d	P_s	λ	γ
0.90	0.99	60	$\{7, 8, 9\}$

Fig.3 gives the average GOSPA, the LEE, the MDE, the FDE, and the SE of the three filters over 100 Monte Carlo runs, and Table 2 shows the average tracking errors and the average running times (RTs) of the three filters. The comparison results are: 1) In terms of tracking accuracy, the TO-MPMBM filter is slightly better than the TPMBM filter, and both the TO-MPMBM filter and TPMBM filter significantly outperform the δ-GLMB filter; 2) In terms of RT, the TO-MPMBM filter is 30.98% and 76.83% lower than the TPMBM filter and the δ-GLMB filter, respectively; 3) The proposed filter unarguably has the best performance in terms of average tracking errors and average RT. The main reason is that the proposed filter propagates the marginal association distributions and PMBM density for each track. It effectively reduces the interference between trajectories by extracting each track and improves the tracking performance. Both the TPMBM filter and the δ-GLMB filter are pruning and merging after updating the joint probability distribution of all trajectories, which lead to an increasing computational burden by retaining a large number of trajectories with low existence probability.

2. The low detection probability scenario

In this scenario, there are 40 time steps, five targets first get close to each other and then split, as shown in Fig.4. Table 3 shows the corresponding parameters that required for the three filters. This scenario aims to test the three algorithms' tracking performance

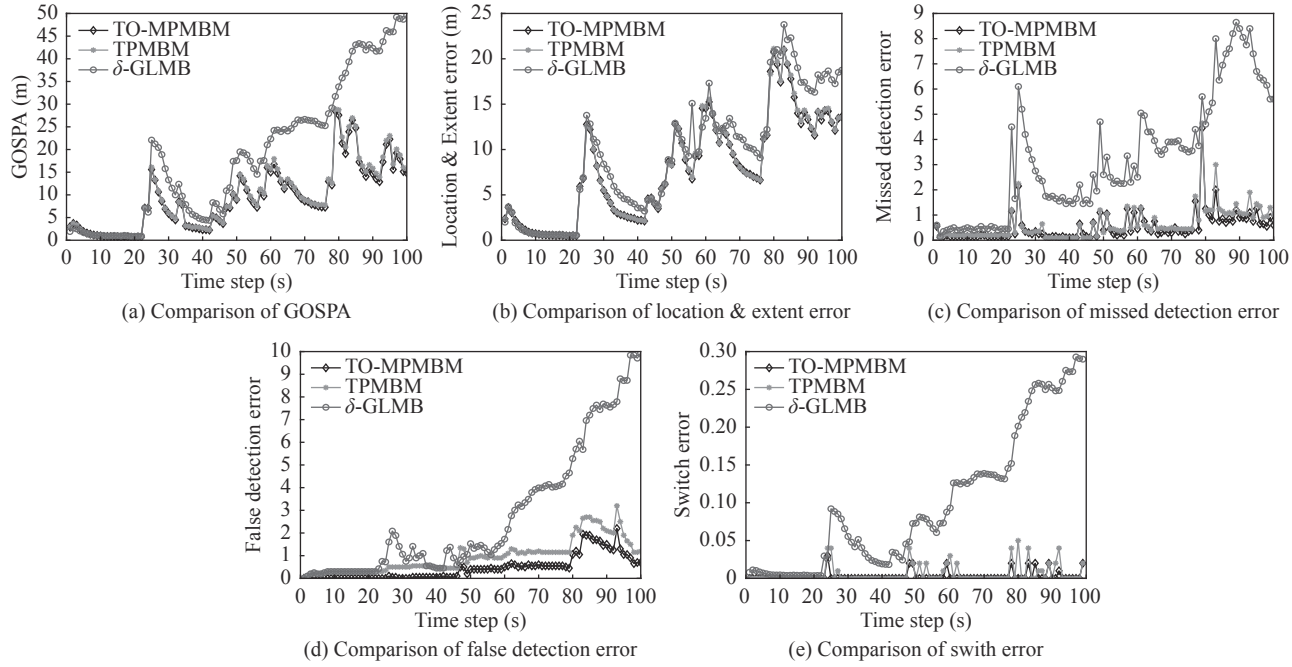

(a) Comparison of GOSPA (b) Comparison of location & extent error (c) Comparison of missed detection error

(d) Comparison of false detection error (e) Comparison of swith error

Fig. 3. Several average errors of three algorithms over 100 Monte Carlo runs (in high clutter scenario).

Table 2. Simulation results of the errors and running time

Parameters	TO-MPMBM	TPMBM	δ-GLMB
GOSPA (m)	927.2	967.6	1912.0
LEE (m)	793.8	799.9	955.1
MDE	53.0	64.9	328.6
FDE	45.4	97.3	280.7
SE	0.2	0.5	9.8
RT (s)	32.3	46.8	139.4

of handling coalescence under low detection probability.

Fig.5 gives the comparisons of the various estimation errors for the three filters over 100 Monte Carlo runs, Table 4 shows the detailed corresponding errors and RTs. Based on Fig.5 and Table 4, the TO-MPMBM filter outperforms the other two filters in terms of average errors and average RTs. At the low detection probability, a large number of measurements not fall within the gate of existing targets. The TO-MPMBM filter re-clusters these measurements and updates them. In addition, the pruned trajectories with low existence probability are recycled into the PPP components and entered into the next prediction, thus avoiding the reduction of trajectories due to missed detection. Therefore, the tracking performance of the TO-MPMBM filter remains good at low detection probability.

Based on the analysis of the two scenarios in the Sections IV.1 and IV.2, the simulation results indicates that the proposed filter performs better than the other filters at low detection probability and high number of clutter.

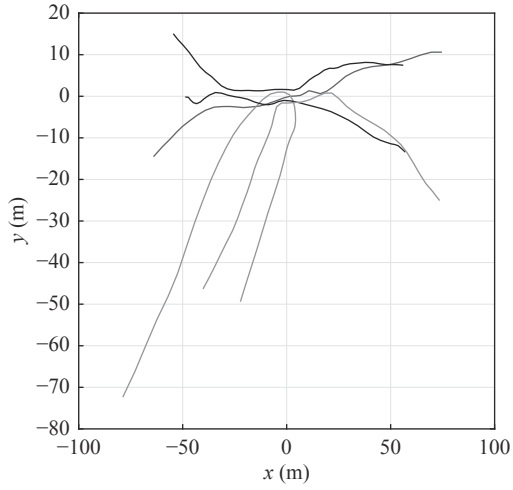

Fig. 4. Target trajectories.

Table 3. The parameters

P_d	P_s	λ	γ
0.70	0.99	10	5

V. Conclusions

In this paper, we propose an efficient GGIW implementation of the TO-MPMBM filter to address the trajectory tracking problem for multiple extended targets. Instead of maintaining the joint posterior PMBM density of the multiple extended target trajectory in the filtering recursion, the TO-MPMBM filter jointly propagates the marginal PMBM density for individual tracks and their existence probabilities. By using individual trajectory distributions to model the uncertainty of in-

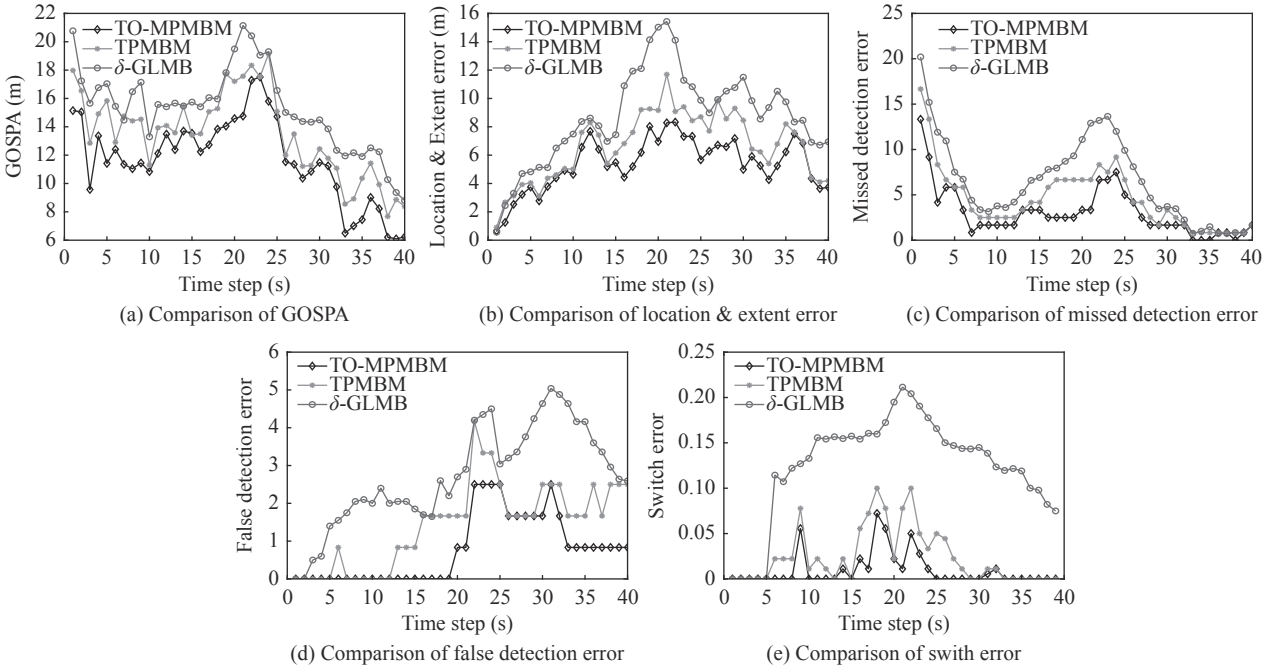

Fig. 5. Several average errors of three algorithms over 100 Monte Carlo runs (in low detection probability scenario).

Table 4. Simulation results of the errors and running time

Parameters	TO-MPMBM	TPMBM	δ-GLMB
GOSPA (m)	467.7	540.3	611.7
LEE (m)	215.7	265.3	349.3
MDE	122.5	182.6	260.4
FDE	30.8	57.5	109.4
SE	0.4	1.0	4.9
RT (m)	6.8	9.3	21.1

dividual target trajectories and using the existence probability of the trajectory distribution to characterize the randomness of target appearance, the proposed filter can deal with an unknown/varying number of targets with uncertain data association, uncertain detection and clutter. The benefits of the proposed filter are twofold. On the one hand, the overall computation is significantly reduced because the Bernoulli components of each track with low existence probability are pruned. On the other hand, the tracking accuracy can be effectively improved by calculating the trajectory marginal PMBM density (instead of the trajectory PMBM density). A comparison of the proposed filter with the existing trajectory filters in two typical scenarios confirms the effectiveness of the proposed filter. Future work includes developing a multi-scan TO-MPMBM filter to solve the multi-scan data association problem.

Appendix A

Proof of Theorem 1 Substituting the p.g.fl. of the multiple extended targets transition density (19) and the p.g.fl. of the trajectory marginal PMBM density (22b) into the p.g.fl. for a trajectory RFS density (7), we find

$$
\begin{aligned}
&G_{k|k-1}[h] \\
&= \int h^{\mathrm{X}} f_{k|k-1}(\mathrm{X})\mathrm{d}\mathrm{X} \\
&= \int\int h^{\mathrm{X}} f^{\mathrm{ali}}_{k|k-1}(\mathrm{X}|\mathrm{X}')\mathrm{d}\mathrm{X} f_{k-1|k-1}(\mathrm{X}')\mathrm{d}\mathrm{X}' \\
&= \exp\left\{\langle D^B_k; h-1\rangle\right\} \int \left(1 - P_{s,k-1} + P_{s,k-1}\langle f^{\mathrm{ali}}; h\rangle\right)^{\mathrm{X}'} \\
&\quad \times f_{k-1|k-1}(\mathrm{X}')\mathrm{d}\mathrm{X}' \\
&= \exp\left\{\langle D^B_k; h-1\rangle\right\} \\
&\quad \times G_{k-1|k-1}\left[1 - P_{s,k-1} + P_{s,k-1}\langle f^{\mathrm{ali}}; h\rangle\right] \\
&\propto \exp\left\{\langle D^B_k; h\rangle\right\} G_{k-1|k-1}\left[1 - P_{s,k-1} + P_{s,k-1}\langle f^{\mathrm{ali}}; h\rangle\right] \\
&= \underbrace{\exp\left\{\langle D^B_k; h\rangle\right\} G^{\mathrm{ppp}}_{k-1|k-1}\left[1 - P_{s,k-1} + P_{s,k-1}\langle f^{\mathrm{ali}}; h\rangle\right]}_{\propto G^{\mathrm{ppp}}_{k|k-1}[h]} \\
&\quad \underbrace{\times G^{\mathrm{mbm}}_{k-1|k-1}\left[1 - P_{s,k-1} + P_{s,k-1}\langle f^{\mathrm{ali}}; h\rangle\right]}_{\propto G^{\mathrm{mbm}}_{k|k-1}[h]}
\end{aligned}
\tag{A-1}
$$

where $G_{k|k-1}[h]$ is the product of two p.g.fl.s that are a PPP component $G^{\mathrm{ppp}}_{k|k-1}[h]$ and an MBM component $G^{\mathrm{mbm}}_{k|k-1}[h]$. The PPP intensity is directly calculated using a standard PHD prediction step (see (22d)). The MBM prediction step is applied to each hypothesis for each trajectory separately (see (9) and (22g)).

$$
\begin{aligned}
&G^{\mathrm{ppp}}_{k|k-1}[h]\\
&\propto \exp\left\{\left\langle D^B_k;h\right\rangle\right\} G^{\mathrm{ppp}}_{k-1|k-1}\left[1-P_{s,k-1}+P_{s,k-1}\left\langle f^{\mathrm{ali}};h\right\rangle\right]\\
&\propto \exp\left\{\left\langle D^B_k;h\right\rangle+\left\langle D^u_{k-1|k-1};1-P_{s,k-1}\right.\right.\\
&\quad \left.\left.+P_{s,k-1}\left\langle f^{\mathrm{ali}};h\right\rangle\right\rangle\right\}\\
&\propto \exp\left\{\langle D^B_k;h\rangle+\langle D^u_{k-1|k-1};P_{s,k-1}\langle f^{\mathrm{ali}};h\rangle\rangle\right\}\\
&=\exp\left\{\langle D^u_{k|k-1};h\rangle\right\}
\end{aligned}
\tag{A-2}
$$

where $\langle D^u_{k|k-1};h\rangle=\langle D^B_k;h\rangle+\langle D^u_{k-1|k-1};P_{s,k-1}\langle f^{\mathrm{ali}};h\rangle\rangle$. Thus $G^{\mathrm{ppp}}_{k|k-1}[h]$ is a PPP and its intensity is given by (25a).

$$
\begin{aligned}
&G^{\mathrm{mbm}}_{k|k-1}[h]\\
&\propto G^{\mathrm{mbm}}_{k-1|k-1}\left[1-P_{s,k-1}+P_{s,k-1}\langle f^{\mathrm{ali}};h\rangle\right]\\
&=\sum_{a\in\mathcal{A}_{k-1|k-1}}\omega^{d,a}\prod_{i\in\mathbb{T}_{k-1|k-1}}G^{d,i,a^i}_{k-1|k-1}\left[1-P_{s,k-1}\right.\\
&\quad\left.+P_{s,k-1}\langle f^{\mathrm{ali}};h\rangle\right]\\
&=\sum_{a\in\mathcal{A}_{k-1|k-1}}\omega^{d,a}\prod_{i\in\mathbb{T}_{k-1|k-1}}G^{d,i,a^i}_{k|k-1}[h]
\end{aligned}
\tag{A-3}
$$

where

$$
\begin{aligned}
&G^{d,i,a^i}_{k|k-1}[h]\\
&=G^{d,i,a^i}_{k-1|k-1}\left[1-P_{s,k-1}+P_{s,k-1}\left\langle f^{\mathrm{ali}};h\right\rangle\right]\\
&=1-r^{d,i,a^i}_{k-1|k-1}+r^{d,i,a^i}_{k-1|k-1}\left\langle f^{d,i,a^i}_{k-1|k-1}\left(X'\right);1-P_{s,k-1}\right.\\
&\quad\left.+P_{s,k-1}\left\langle f^{\mathrm{ali}};h\right\rangle\right\rangle\\
&=1-r^{d,i,a^i}_{k-1|k-1}+r^{d,i,a^i}_{k-1|k-1}\int f^{d,i,a^i}_{k-1|k-1}\left(X'\right)\left(1-P_{s,k-1}\right.\\
&\quad\left.+P_{s,k-1}\int f^{\mathrm{ali}}\left(X\mid X'\right)h(X)\left\langle f^{\mathrm{ali}};h\right\rangle\right)\mathrm{d}X\mathrm{d}X'\\
&=1-r^{d,i,a^i}_{k-1|k-1}+r^{d,i,a^i}_{k-1|k-1}\left(\int\left(1-P_{s,k-1}\right)f^{d,i,a^i}_{k-1|k-1}\left(X'\right)\mathrm{d}X'\right.\\
&\quad\left.+\iint f^{\mathrm{ali}}\left(X\mid X'\right)h(X)\mathrm{d}XP_{s,k-1}f^{d,i,a^i}_{k-1|k-1}\left(X'\right)\mathrm{d}X'\right)\\
&=1-r^{d,i,a^i}_{k|k-1}+r^{d,i,a^i}_{k|k-1}\int h(X)f^{d,i,a^i}_{k|k-1}(X)\mathrm{d}X
\end{aligned}
\tag{A-4}
$$

where $r^{d,i,a^i}_{k|k-1}$ and $f^{d,i,a^i}_{k|k-1}(\cdot)$ in the last equality can be obtained via (25e) and (25f). According to (A-3) and (A-4), we obtain that the form $G^{\mathrm{mbm}}_{k|k-1}[h]$ is similar to (22g), with $n_{k|k-1}=n_{k-1|k-1}$, $h^i_{k|k-1}=h^i_{k-1|k-1}$, and $\omega^{d,i,a^i}_{k|k-1}=\omega^{d,i,a^i}_{k-1|k-1},\forall a^i$.

Appendix B

Any p.g.fl of the following form is an unnormalised Bernoulli distribution, see [15]:

$$
a+\langle b;h\rangle=\omega(1-r+r\langle f;h\rangle)
\tag{B-1}
$$

where

$$
\omega=a+\int b(x)\mathrm{d}x
\tag{B-2}
$$

$$
r=\frac{\int b(x)\mathrm{d}x}{a+\int b(x)\mathrm{d}x}
\tag{B-3}
$$

$$
f(x)=\frac{b(x)}{\int b(x)\mathrm{d}x}
\tag{B-4}
$$

Appendix C

Suppose set-parameterised functionals is $F^{W_i}_{\tilde{a},i}[g;h]=\frac{\mathrm{d}F_{\tilde{a},i}}{\mathrm{d}W_i}[g;h]$, $i\in\{0,1,\ldots,n\}$, such that $F^{W_0}_{\tilde{a},0}=\prod_{\mathrm{w}\in W_0}f^{w}_{\tilde{a},0}[g;h]$. If $\mathrm{Z}_k=\{\mathrm{w}^p_k|p\in\{1,\ldots,|\mathcal{P}(\mathrm{Z}_k)|-1\}$, then

$$
\begin{aligned}
&\sum_{W_0\uplus W_1\uplus\ldots\uplus W_n=\mathrm{Z}_k}\frac{\mathrm{d}F_{\tilde{a},0}}{\mathrm{d}W_0}[g;h]\frac{\mathrm{d}F_{\tilde{a},1}}{\mathrm{d}W_1}[g;h]\cdots\frac{\mathrm{d}F_{\tilde{a},n}}{\mathrm{d}W_n}[g;h]\\
&=\sum_{W_0\uplus W_1\uplus\cdots\uplus W_n=\mathrm{Z}_k}\prod_{i=0}^{n}F^{W_i}_{\tilde{a},i}[g;h]\\
&=\sum_{\bar{a}\in\mathcal{A}_k}\prod_{i=1}^{n+|\mathcal{P}(\mathrm{Z}_k)|-1}F^{\mathrm{Z}^{\bar{a}^i}}_{\tilde{a},i}[g;h]
\end{aligned}
\tag{C-1}
$$

where

$$
\begin{aligned}
\mathcal{A}_k=&\{(\bar{a}^1,\bar{a}^2,\ldots,\bar{a}^{n+|\mathcal{P}(\mathrm{Z}_k)|-1})|\bar{a}^i\in\{0,1,\ldots,|\mathcal{P}(\mathrm{Z}_k)|-1\},\\
&\text{for } i\in\{1,\ldots,n\},\ \bar{a}^{n+j}\in\{0,j\},\text{for } j\in\{1,\ldots,|\mathcal{P}(\mathrm{Z}_k)|-1\},\\
&\textstyle\bigcup_{i=1}^{n+|\mathcal{P}(\mathrm{Z}_k)|-1}\mathcal{M}_k(i,\bar{a}^i)=\{(k,j_1),(k,j_2),\ldots,(k,j_{|\mathrm{w}^p_k|})\},\\
&\mathcal{M}_k(i,\bar{a}^i)\cap\mathcal{M}_k(j,\bar{a}^j)=\emptyset,\ \forall i\neq j\}
\end{aligned}
\tag{C-2}
$$

with $\mathcal{M}_k(i,0)=\emptyset$ and $\mathcal{M}_k(i,j)=\{k,j\}$. Finally

$$
\mathrm{Z}^{\bar{a}^i}=\begin{cases}0, & \bar{a}^i=0\\ \left(\mathrm{w}^p_k\right)^{\bar{a}^i}, & \bar{a}^i=\{1,\ldots,|\mathcal{P}\left(\mathrm{Z}_k\right)|-1\}\end{cases}
\tag{C-3}
$$

and for $j\in\{1,\ldots,|\mathcal{P}(\mathrm{Z}_k)|-1\}$

$$
F^{W_i}_{\tilde{a},i}[g;h]=\begin{cases}1, & |W_i|=1\\ f^{\mathrm{w}}_{\tilde{a},i}[g;h], & |W_i|>1\end{cases}
\tag{C-4}
$$

The above proof details in [15].

Appendix D

Proof of Theorem 2 Substituting the measurement p.g.fl (21) and the p.g.fl of the trajectory marginal PMBM density (22b) into the p.g.fl for a trajectory RFS density (7), we find

$$
\begin{aligned}
&G_{k|k}[h] \\
&= \int h^{\mathrm{X}} f_{k|k}(\mathrm{X})\mathrm{dX} \\
&\propto \int h^{\mathrm{X}} f(\mathrm{Z}_k|\mathrm{X}) f_{k|k-1}(\mathrm{X})\mathrm{dX} \\
&= \frac{\mathrm{d}}{\mathrm{dZ}_k}\left(\int\int h^{\mathrm{X}} g^{\mathrm{Z}_k} f(\mathrm{Z}_k|\mathrm{X}) f_{k|k-1}(\mathrm{X})\mathrm{dX}\mathrm{dZ}_k\right)\Big|_{g=0} \\
&= \frac{\mathrm{d}}{\mathrm{dZ}_k}\left(\int h^{\mathrm{X}} G[g|\mathrm{X}] f_{k|k-1}(\mathrm{X})\mathrm{dX}\right)\Big|_{g=0} \\
&= \frac{\mathrm{d}}{\mathrm{dZ}_k}\left(\exp\left\{\langle \lambda_k^{\mathrm{FA}}; g-1\rangle\right\}\int h^{\mathrm{X}}(1-P_d+P_d\langle\phi;g\rangle)^{\mathrm{X}}\right. \\
&\quad \left.\times\ f_{k|k-1}(\mathrm{X})\mathrm{dX}\right)\big|_{g=0} \\
&= \frac{\mathrm{d}}{\mathrm{dZ}_k}\left(\exp\left\{\langle \lambda_k^{\mathrm{FA}}; g-1\rangle\right\} G_{k|k-1}\left[h(1-P_d+P_d\langle\phi;g\rangle)\right]\right)\Big|_{g=0} \\
&\propto \frac{\mathrm{d}}{\mathrm{dZ}_k}(\exp\left\{\langle \lambda_k^{\mathrm{FA}}; g\rangle\right\} G^{\mathrm{PPP}}_{k|k-1}\left[h(1-P_d+P_d\langle\phi;g\rangle)\right] \\
&\quad \times G^{\mathrm{mbm}}_{k|k-1}\left[h(1-P_d+P_d\langle\phi;g\rangle)\right])\Big|_{g=0} \\
&\propto \frac{\mathrm{d}}{\mathrm{dZ}_k}(\exp\left\{\langle \lambda_k^{\mathrm{FA}}; g\rangle + \langle D^u_{k|k-1}; h(1-P_d+P_d\langle\phi;g\rangle)\rangle\right\} \\
&\quad \times G^{\mathrm{mbm}}_{k|k-1}\left[h(1-P_d+P_d\langle\phi;g\rangle)\right])\Big|_{g=0} \\
&= \underbrace{\exp\left\{\langle D^u_{k|k-1}; h(1-P_d)\rangle\right\}}_{\propto G^{\mathrm{PPP}}_{k|k}[h]} \frac{\mathrm{d}}{\mathrm{dZ}_k}(\exp\{\langle \lambda_k^{\mathrm{FA}}; g\rangle \\
&\quad + \langle D^u_{k|k-1}; hP_d\langle\phi;g\rangle\rangle\} G^{\mathrm{mbm}}_{k|k-1}\left[h(1-P_d+P_d\langle\phi;g\rangle)\right])\Big|_{g=0}
\end{aligned}
\tag{D-1}
$$

with

$$
G^{\mathrm{PPP}}_{k|k}[h] = \exp\left\{\langle D^u_{k|k-1}; h(1-P_d)\rangle\right\} \tag{D-2}
$$

$$
G^{\mathrm{mbm-P}}_{k|k}[h] = \tfrac{\mathrm{d}}{\mathrm{dZ}_k}\exp\left\{\langle \lambda_k^{\mathrm{FA}}; g\rangle + \langle D^u_{k|k-1}; hP_d\langle\phi;g\rangle\rangle\right\}\Big|_{g=0} \tag{D-3}
$$

$$
G^{\mathrm{mbm-b}}_{k|k}[h] = \tfrac{\mathrm{d}}{\mathrm{dZ}_k} G^{\mathrm{mbm}}_{k|k-1}\left[h(1-P_d+P_d\langle\phi;g\rangle)\right]\Big|_{g=0} \tag{D-4}
$$

$$
G^{\mathrm{mbm}}_{k|k}[h] = G^{\mathrm{mbm-P}}_{k|k}[h] G^{\mathrm{mbm-b}}_{k|k}[h] \tag{D-5}
$$

where $G_{k|k}[h]$ is the product of two p.g.fls which are a PPP component $G^{\mathrm{ppp}}_{k|k}[h]$ and an MBM component $G^{\mathrm{mbm}}_{k|k}[h]$. The PPP intensity is directly calculated using a standard PHD update step (22d) and arrived at the result in (26). The MBM p.g.fl ($G^{\mathrm{mbm}}_{k|k}[h]$) consists of two steps: 1) updating the detected portion of the PPP with PPP-distribution clutter ($G^{\mathrm{mbm-P}}_{k|k}[h]$), and 2) updating the Bernoulli component ($G^{\mathrm{mbm-b}}_{k|k}[h]$).

Using the derivative of a linear function and the chain rule in [6], we get

$$
\tfrac{\mathrm{d}}{\mathrm{d}z}\langle f; g\rangle = f(z) \tag{D-6}
$$

$$
\tfrac{\mathrm{d}}{\mathrm{d}z} f(F[g]) = \tfrac{\mathrm{d}}{\mathrm{d}z}F[g]\tfrac{\mathrm{d}}{\mathrm{d}y}f(y)\Big|_{y=F[g]} \tag{D-7}
$$

So,

$$
\begin{aligned}
&\frac{\mathrm{d}}{\mathrm{d}z}\exp\left\{\langle \lambda_k^{\mathrm{FA}}; g\rangle + \langle D^u_{k|k-1}; hP_d\langle\phi;g\rangle\rangle\right\} \\
&= \exp\left\{\langle \lambda_k^{\mathrm{FA}}; g\rangle + \langle D^u_{k|k-1}; hP_d\langle\phi;g\rangle\rangle\right\} \\
&\quad \times \frac{\mathrm{d}}{\mathrm{d}z}\left(\langle \lambda_k^{\mathrm{FA}}; g\rangle + \langle D^u_{k|k-1}; hP_d\langle\phi;g\rangle\rangle\right) \\
&= \exp\left\{\langle \lambda_k^{\mathrm{FA}}; g\rangle + \langle D^u_{k|k-1}; hP_d\langle\phi;g\rangle\rangle\right\} \\
&\quad \times \left(\frac{\mathrm{d}}{\mathrm{d}z}\langle \lambda_k^{\mathrm{FA}}; g\rangle + \frac{\mathrm{d}}{\mathrm{d}z}\langle D^u_{k|k-1}; hP_d\langle\phi;g\rangle\rangle\right) \\
&= \exp\left\{\langle \lambda_k^{\mathrm{FA}}; g\rangle + \langle D^u_{k|k-1}; hP_d\langle\phi;g\rangle\rangle\right\} \\
&\quad \times \left(\lambda_k^{\mathrm{FA}}(z) + \langle D^u_{k|k-1}; hP_d\phi(z|\cdot)\rangle\right)
\end{aligned}
\tag{D-8}
$$

Iterating the derivative of (D-8), we find

$$
\begin{aligned}
&G^{\mathrm{mbm-P}}_{k|k}[h] \\
&= \frac{\mathrm{d}}{\mathrm{d}\mathbf{Z}_k}\exp\left\{\langle \lambda_k^{\mathrm{FA}}; g\rangle + \langle D^u_{k|k-1}; hP_d\langle\phi;g\rangle\rangle\right\}\Big|_{g=0} \\
&= \left(\exp\left\{\langle \lambda_k^{\mathrm{FA}}; g\rangle + \langle D^u_{k|k-1}; hP_d\langle\phi;g\rangle\rangle\right\}\right. \\
&\quad \left.\times \prod_{z_k\in\mathbf{Z}_k}\left(\lambda_k^{\mathrm{FA}}(z_k) + \langle D^u_{k|k-1}; hP_d\phi(z_k|\cdot)\rangle\right)\right)\Big|_{g=0} \\
&= \prod_{z_k\in\mathrm{Z}_k}\omega^{z_k}_{k|k}\left(1-r^{z_k}_{k|k}+r^{z_k}_{k|k}\langle f^{z_k}_{k|k}; h\rangle\right)
\end{aligned}
\tag{D-9}
$$

The Bayes update of an unnormalised Poisson distribution in Poisson clutter can be obtained via (D-9). $\omega^{z_k}_{k|k}$, $r^{z_k}_{k|k}$ and $f^{z_k}_{k|k}(\cdot)$ (which are calculated using Appendix B are given in (D-4)–(D-6), respectively.

Using (22b), (22g), and Appendix C, we find

$$
\begin{aligned}
&G^{\mathrm{mbm}}_{k|k}[h] \\
&= \frac{\mathrm{d}}{\mathrm{dZ}_k}\left(\exp\left\{\langle \lambda_k^{\mathrm{FA}}; g\rangle + \langle D^u_{k|k-1}; hP_d\langle\phi;g\rangle\rangle\right\}\right. \\
&\quad \left.\times \sum_{\tilde{a}\in\mathcal{A}_{k|k-1}}\omega^{d,\tilde{a}}\prod_{i\in\mathbb{T}_{k|k-1}} G^{d,i,\tilde{a}^i}_{k|k-1}\left[h(1-P_d+P_d\langle\phi;g\rangle)\right]\right)\Big|_{g=0} \\
&\propto \frac{\mathrm{d}}{\mathrm{dZ}_k}\left(\exp\left\{\langle \lambda_k^{\mathrm{FA}}; g\rangle + \langle D^u_{k|k-1}; hP_d\langle\phi;g\rangle\rangle\right\}\right. \\
&\quad \left.\times \sum_{\tilde{a}\in\mathcal{A}_{k|k-1}}\prod_{i\in\mathbb{T}_{k|k-1}}\omega^{d,i,\tilde{a}^i}_{k|k-1} G\left[h(1-P_d+P_d\langle\phi;g\rangle)\right]\right)\Big|_{g=0} \\
&= \sum_{\tilde{a}\in\mathcal{A}_{k|k-1}}\frac{\mathrm{d}}{\mathrm{dZ}_k}\left(\exp\left\{\langle \lambda_k^{\mathrm{FA}}; g\rangle + \langle D^u_{k|k-1}; hP_d\langle\phi;g\rangle\rangle\right\}\right. \\
&\quad \left.\times \prod_{i\in\mathbb{T}_{k|k-1}}\omega^{d,i,\tilde{a}^i}_{k|k-1} G\left[h(1-P_d+P_d\langle\phi;g\rangle)\right]\right)\Big|_{g=0} \\
&= \sum_{\tilde{a}\in\mathcal{A}_{k|k-1}}\sum_{W_0\uplus W_1\uplus\ldots\uplus W_n=\mathrm{Z}_k}\frac{\mathrm{d}F_{\tilde{a},0}}{\mathrm{d}W_0}[g;h]\frac{\mathrm{d}F_{\tilde{a},1}}{\mathrm{d}W_1}[g;h] \\
&\quad \times\cdots\times\frac{\mathrm{d}F_{\tilde{a},n}}{\mathrm{d}W_n}[g;h]\Big|_{g=0} \\
&= \sum_{\tilde{a}\in\mathcal{A}_{k|k-1}}\sum_{\bar{a}\in\mathcal{A}_k}\prod_{i=1}^{n+|\mathcal{P}(\mathrm{Z}_k)|-1} F^{\mathrm{Z}^{\bar{a}^i}}_{\tilde{a},i}[g;h]\Big|_{g=0} \\
&= \sum_{\tilde{a}\in\mathcal{A}_{k|k-1},\bar{a}\in\mathcal{A}_k}\prod_{i=1}^{n+|\mathcal{P}(\mathrm{Z}_k)|-1} F^{\mathrm{Z}^{\bar{a}^i}}_{\tilde{a},i}[g;h]\Big|_{g=0}
\end{aligned}
\tag{D-10}
$$

where

$$F_{\tilde{a},0}[g;h]=\exp\left\{\langle\lambda_k^{\mathrm{FA}};g\rangle+\langle D_{k|k-1}^{u};hP_d\langle\phi;g\rangle\rangle\right\} \tag{D-11}$$

$$F_{\tilde{a},i}[g;h]=\omega_{k|k-1}^{d,i,\tilde{a}^i}G\left[h(1-P_d+P_d\langle\phi;g\rangle)\right],i>0 \tag{D-12}$$

As the set of events $a\in\mathcal{A}_{k|k}$ covers the same as events $\tilde{a}\in\mathcal{A}_{k|k-1}$ and $\bar{a}\in\mathcal{A}_k$ $(\mathcal{M}_k(i,a^i)=\mathcal{M}_{k-1}(i,\tilde{a}^i)\cup\mathcal{M}_k(i,\bar{a}^i))$, the formula (D-10) can be rewritten as

$$G_{k|k}^{\mathrm{mbm}}[h]\propto\sum_{a\in\mathcal{A}_{k|k}}\prod_{i=1}^{n+|\mathcal{P}(Z_k)|-1}F_{\tilde{a},i}^{Z^{\bar{a}^i}}[g;h]\Big|_{g=0} \tag{D-13}$$

Using (D-10), (9) and Appendix B, we find

$$\begin{aligned}
&F_{\tilde{a},i}^{Z^{\bar{a}^i}}[g;h]\Big|_{g=0}\\
&\propto\frac{\mathrm{d}}{\mathrm{d}Z_k}\left(\omega_{k|k-1}^{d,i,\tilde{a}^i}G\left[h(1-P_d+P_d\langle\phi;g\rangle)\right]\right)\Big|_{g=0}\\
&=\frac{\mathrm{d}}{\mathrm{d}Z_k}(\omega_{k|k-1}^{d,i,\tilde{a}^i}(1-r_{k|k-1}^{d,i,\tilde{a}^i}\\
&\quad+r_{k|k-1}^{d,i,\tilde{a}^i}\langle f_{k|k-1}^{d,i,\tilde{a}^i};h(1-P_d+P_d\langle\phi;g\rangle)\rangle))\Big|_{g=0}\\
&=\frac{\mathrm{d}}{\mathrm{d}Z_k}(\omega_{k|k-1}^{d,i,\tilde{a}^i}(1-r_{k|k-1}^{d,i,\tilde{a}^i}+r_{k|k-1}^{d,i,\tilde{a}^i}(\langle f_{k|k-1}^{d,i,\tilde{a}^i};h(1-P_d)\rangle\\
&\quad+\langle f_{k|k-1}^{d,i,\tilde{a}^i};hP_d\langle\phi;g\rangle\rangle)))\Big|_{g=0}\\
&=\omega_{k|k}^{d,i,a^i}\left(1-r_{k|k}^{d,i,a^i}+r_{k|k}^{d,i,a^i}\langle f_{k|k}^{d,i,a^i};h\rangle\right)\\
&=\omega_{k|k}^{d,i,a^i}G_{k|k}^{d,i,a^i}[h]
\end{aligned} \tag{D-14}$$

where $\omega_{k|k}^{d,i,a^i}$, $r_{k|k}^{d,i,a^i}$ and $f_{k|k}^{d,i,a^i}(\cdot)$ are given in (29c)–(29e) (detections updating existing tracks with nonempty measurement set w_k^p, i.e., $i\in\{1,\ldots,n_{k|k-1}\}$, $\tilde{a}^i\in\{1,\ldots,h_{k|k-1}^i\}$, $a^i=\tilde{a}^i+h_{k|k-1}^i p$), (30b)–(30d) (missed detections on existing tracks, i.e., $i\in\{1,\ldots,n_{k|k-1}\}$, $a^i\in\{1,\ldots,h_{k|k-1}^i\}$), (31b) (new tracks without measurements, i.e., $i\in\{n_{k|k-1}+p\}$, $a^i=1$) and (31d)–(31f) (updating of new tracks, i.e., $i\in\{n_{k|k-1}+p\}$, $a^i=2$).

References

[1] B. N. Vo, M. Mallick, Y. Bar-shalom, *et al.*, "Multitarget tracking," in *Wiley Encyclopedia of Electrical and Electronics Engineering*, J. G. Webster, Ed. Wiley, New York, NY, USA, 2020.

[2] B. Yang, S. Q. Zhu and X. P. He, "IMM Robust Cardinality Balance Multi-Bernoulli Filter for Multiple Maneuvering Target Tracking with Interval Measurement," *Chinese Journal of Electronics*, vol.30, no.6, pp.1141–1151, 2021.

[3] K. Granström, M. Baum, and S. Reuter, "Extended object tracking: introduction, overview, and applications," *Journal of Advances in Information Fusion*, vol.12, no.2, pp.139–174, 2017.

[4] K. Gilholm, S. Godsill, S. Maskell, *et al.*, "Poisson models for extended target and group tracking," in *Proceedings of SPIE 5913, Signal and Data Processing of Small Targets 2005*, San Diego, CA, USA, article no.59130R, 2005.

[5] K. Gilholm and D. Salmond, "Spatial distribution model for tracking extended objects," *IEE Proceedings - Radar, Sonar and Navigation*, vol.152, no.5, pp.364–371, 2005.

[6] R. P. S. Mahler, *Statistical Multisource-Multitarget Information Fusion*. Artech House, Boston, MA, USA, pp.1–48, 2007.

[7] K. Granstrom and U. Orguner, "A phd filter for tracking multiple extended targets using random matrices," *IEEE Transactions on Signal Processing*, vol.60, no.11, pp.5657–5671, 2012.

[8] C. Lundquist, K. Granström, and U. Orguner, "An extended target CPHD filter and a gamma Gaussian inverse wishart implementation," *IEEE Journal of Selected Topics in Signal Processing*, vol.7, no.3, pp.472–483, 2013.

[9] M. Beard, S. Reuter, K. Granström, *et al.*, "A generalised labelled multi-Bernoulli filter for extended multi-target tracking," in *Proceedings of 2015 18th International Conference on Information Fusion (Fusion)*, Washington, DC, USA, pp.991–998, 2015.

[10] M. Beard, S. Reuter, K. Granström, *et al.*, "Multiple extended target tracking with labeled random finite sets," *IEEE Transactions on Signal Processing*, vol.64, no.7, pp.1638–1653, 2016.

[11] K. Granström, M. Fatemi, and L. Svensson, "Poisson multibernoulli mixture conjugate prior for multiple extended target filtering," *IEEE Transactions on Aerospace and Electronic Systems*, vol.56, no.1, pp.208–225, 2020.

[12] B. T. Vo and B. N. Vo, "Labeled random finite sets and multi-object conjugate priors," *IEEE Transactions on Signal Processing*, vol.61, no.13, pp.3460–3475, 2013.

[13] L. Cament, J. Correa, M. Adams, *et al.*, "The histogram Poisson, labeled multi-Bernoulli multi-target tracking filter," *Signal Processing*, vol.176, article no.107714, 2020.

[14] X. L. Wang, W. X. Xie, and L. Q. Liang, "Labeled Multi-Bernoulli Maneuvering Target Tracking Algorithm via TSK Iterative Regression Model," *Chinese Journal of Electronics*, vol.31, no.2, article no.pp. 227—239, 2022.

[15] J. L. Williams, "Marginal multi-bernoulli filters: RFS derivation of MHT, JIPDA, and association-based member," *IEEE Transactions on Aerospace and Electronic Systems*, vol.51, no.3, pp.1664–1687, 2015.

[16] Á. F. García-Fernández, J. L. Williams, K. Granström, *et al.*, "Poisson multi-bernoulli mixture filter: direct derivation and implementation," *IEEE Transactions on Aerospace and Electronic Systems*, vol.54, no.4, pp.1883–1901, 2018.

[17] K. Granström, L. Svensson, Y. X. Xia, *et al.*, "Poisson multi-bernoulli mixture trackers: continuity through random finite sets of trajectories," in *Proceedings of 2018 21st International Conference on Information Fusion (FUSION)*, Cambridge, UK, pp.1–5, 2018.

[18] L. Svensson and M. Morelande, "Target tracking based on estimation of sets of trajectories," in *Proceedings of the 17th International Conference on Information Fusion (FUSION)*, Salamanca, Spain, pp.1–8, 2014.

[19] Á. F. García-Fernández, L. Svensson, and M. R. Morelande, "Multiple target tracking based on sets of trajectories," *IEEE Transactions on Aerospace and Electronic Systems*, vol.56, no.3, pp.1685–1707, 2020.

[20] Y. X. Xia, K. Granström, L. Svensson, *et al.*, "Extended target Poisson multi-Bernoulli mixture trackers based on sets of trajectories," in *Proceedings of 2019 22th International Conference on Information Fusion (FUSION)*, Ottawa, ON, Canada, pp.1–8, 2019.

[21] H. C. Du and W. X. Xie, "Extended target marginal distribution Poisson multi-bernoulli mixture filter," *Sensors*, vol.20, no.18, article no.5387, 2020.

[22] R. P. S. Mahler, Advances in Statistical Multisource-Multitarget Information Fusion. Artech House, Boston, MA, USA,

2014.

[23] M. Feldmann and D. Franken, "Tracking of extended objects and group targets using random matrices—a new approach," in *Proceedings of 2008 11th International Conference on Information Fusion*, Cologne, Germany, pp.1–8, 2008.

[24] K. Granström and U. Orguner, "New prediction for extended targets with random matrices," *IEEE Transactions on Aerospace and Electronic Systems*, vol.50, no.2, pp.1577–1589, 2014.

[25] J. Lan and X. R. Li., "Extended-object or group-target tracking using random matrix with nonlinear measurements," *IEEE Transactions on Signal Processing*, vol.67, no.19, pp.5130–5142, 2019.

[26] L. Gao, Z. L. Jing, M. Z. Li, *et al.*, "Bayesian approach to multiple extended targets tracking with random hypersurface models," *IET Radar, Sonar & Navigation*, vol.13, no.4, pp.601–611, 2019.

[27] M. Baum and U. D. Hanebeck, "Random Hypersurface Models for extended object tracking," in *Proceedings of 2009 IEEE International Symposium on Signal Processing and Information Technology (ISSPIT)*, Ajman, United Arab Emirates, pp.178–183, 2009.

[28] N. Wahlström and E. Özkan, "Extended target tracking using Gaussian processes," *IEEE Transactions on Signal Processing*, vol.63, no.16, pp.4165–4178, 2015.

[29] K. Granström, L. Svensson, S. Reuter, *et al.*, "Likelihood-based data association for extended object tracking using sampling methods," *IEEE Transactions on Intelligent Vehicles*, vol.3, no.1, pp.30–45, 2018.

[30] K. G. Murty, "Letter to the Editor—An algorithm for ranking all the assignments in order of increasing cost," *Operations Research*, vol.16, no.3, pp.682–687, 1968.

[31] K. Granström, S. Renter, M. Fatemi, *et al.*, "Pedestrian tracking using Velodyne data—Stochastic optimization for extended object tracking," in *Proceedings of 2017 IEEE Intelligent Vehicles Symposium (IV)*, Los Angeles, CA, USA, pp.39–46, 2017.

[32] M. Fatemi, K. Granström, L. Svensson, *et al.*, "Poisson multi-bernoulli mapping using Gibbs sampling," *IEEE Transactions on Signal Processing*, vol.65, no.11, pp.2814–2827, 2017.

[33] K. Granström, M. Fatemi, and L. Svensson, "Gamma Gaussian inverse-Wishart Poisson multi-Bernoulli filter for extended target tracking," in *Proceedings of 2016 19th International Conference on Information Fusion (FUSION)*, Heidelberg, Germany, pp.893–900, 2016.

[34] A. S. Rahmathullah, Á. F. García-Fernández, and L. Svensson, "Generalized optimal sub-pattern assignment metric," in *Proceedings of 2017 20th International Conference on Information Fusion (Fusion)*, Xi'an, China, pp.1–8, 2017.

[35] S. S. Yang, M. Baum, and K. Granström, "Metrics for performance evaluation of elliptic extended object tracking methods," in *Proceedings of 2016 IEEE International Conference on Multisensor Fusion and Integration for Intelligent Systems (MFI)*, Baden-Baden, Germany, pp.523–528, 2017.

DU Haocui was born in 1986. She reveived the Ph.D. degree from Shenzhen University, Shenzhen, China. Her main research interests include radar target tracking and intelligent information processing.
(Email: hcdu@szu.edu.cn)

XIE Weixin was born in 1941. He received the B.S. degree from Xidian University, Xi'an, China, and joined the faculty of Xidian University in 1965. From 1981 to 1983, he was a Visiting Scholar with University of Pennsylvania, USA. In 1989, he was invited to University of Pennsylvania as a Visiting Professor. He is currently a Professor with Shenzhen University. His main research interests include intelligent information processing, fuzzy information processing, image processing, and pattern recognition. (Email: wxxie@szu.edu.cn)

LIU Zongxiang (corresponding author) was born in 1965. He received the Ph.D. degree from Xidian University, Xi'an, China. He is currently a Professor of College of Electronic and Information Engineering, Shenzhen University. His research interests include multi-sensor information fusion, multiple target tracking, and random set theory.
(Email: liuzx@szu.edu.cn)

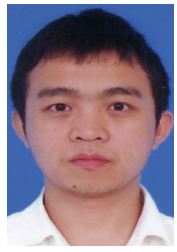

LI Liangqun was born in 1979. He is currently a Professor of College of Information Engineering, Shenzhen University. He visited the University of New Orleans (UNO) as a Visiting Research Scientist from 2017 to 2018. His research interests include signal processing, fuzzy sets, information fusion, and target tracking. (Email: lqli@szu.edu.cn)